JOC Article

Fluorescence Sensing of Anions Based on Inhibition of Excited-State Intramolecular Proton Transfer

Yunkou Wu, Xiaojun Peng,* Jiangli Fan, Shang Gao, Maozhong Tian, Jianzhang Zhao, and Shiguo Sun

State Key Laboratory of Fine Chemicals, Dalian University of Technology, 158 Zhongshan Road, Dalian 116012, People's Republic of China

pengxj@dlut.edu.cn

Received August 5, 2006

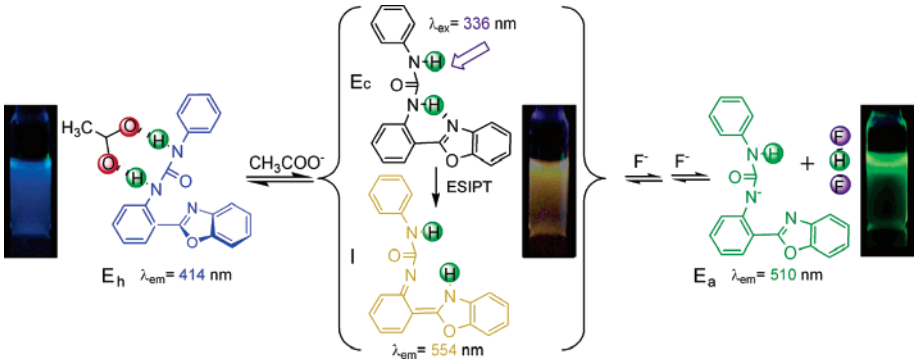

Condensation of 2-(2′-aminophenyl)benzoxazole with *p*-toluenesulfonyl chloride and phenyl isocyanate yields two new anion sensors (TABO and PUBO), which can undergo excited-state intramolecular proton transfer (ESIPT) upon excitation. For the acid receptor TABO, the ESIPT process can be readily disturbed by basic anions such as F^-, CH_3COO^-, and $H_2PO_4^-$ by deprotonating the sulfonamide unit, whereas in the case of PUBO, a good hydrogen-bonding donor, the ESIPT process is inhibited either by the fluoride-induced deprotonation of the urea unit or by the formation of a strong CH_3COO^-−urea intermolecular hydrogen bond complex, and these two types of inhibition mechanisms consequently result in different ratiometric responses. But other anions with less hydrogen-bonding acceptor abilities cannot inhibit the ESIPT. Interestingly, the different inhibition abilities of F^-, CH_3COO^-, and $H_2PO_4^-$ produce different spectral behaviors in PUBO, so this new sensor successfully distinguishes the subtle difference in these three anionic substrates of similar basicity and surface charge density.

Introduction

A great deal of attention has recently been focused on the selective sensing of anions by means of synthetic receptors because of the fundamental roles of anions in many chemical and biological processes.[1] In order to selectively differentiate between biologically interesting anionic substrates of similar basicity and surface charge density, such as F^-, CH_3COO^-, and $H_2PO_4^-$, considerable efforts have been made to develop hydrogen-bonding donors/receptors containing urea,[2] thiourea,[3] amide,[4] phenol,[5] imidazole ion,[6] or pyrrole[7] subunits and to utilize different kinds of signaling mechanisms including internal charge transfer (ICT),[8] photoinduced electron transfer (PET),[9]

(1) (a) Schrader, T., Hamilton, A. D., Eds. *Functional Synthetic Receptors*; Wiley-VCH: Weinheim, Germany, 2005. (b) *Anion Sensing*; Stibor, I., Ed.; Topics in Current Chemistry 255; Springer-Verlag: Berlin, Heidelberg, New York, 2005. (c) Gale, P. A., Ed. *Coord. Chem. Rev.* **2003**, *240*, 1−2. (d) Martinez-Manez, R.; Sancenon, F. *Chem. Rev.* **2003**, *103*, 4419−4476. (e) Sessler, J. L.; Davis, J. M. *Acc. Chem. Res.* **2001**, *34*, 989−997.

(2) (a) Esteban-Gomez, D.; Fabbrizzi, L.; Liechelli, M. *J. Org. Chem.* **2005**, *70*, 5717−5720. (b) Cho, E. J.; Ryu, B. J.; Lee, Y. J.; Nam, K. C. *Org. Lett.* **2005**, *7*, 2607−2609. (c) Descalzo, A. B.; Rurack, K.; Weisshoff, H.; Martinez-Manez, R.; Marcos, M. D.; Amoros, P.; Hoffmann, K.; Soto, J. *J. Am. Chem. Soc.* **2005**, *127*, 184−200. (d) Cho, E. J.; Moon, J. W.; Ko, S. W.; Lee, J. Y.; Kim, S. K.; Yoon, J.; Nam, K. C. *J. Am. Chem. Soc.* **2003**, *125*, 12376−12377.

10.1021/jo061634c CCC: $37.00
Published on Web 12/05/2006

metal-to-ligand charge transfer (MLCT),[10] excimer/exciplex formation,[4a,11] and tuning proton transfer[12] for fluorescence chemosensors. But the differentiation is always poor due to the same spectral outputs for the anion−receptor interactions.[5c] Here we report two new anion fluorescence chemosensors based on inhibition of the excited-state intramolecular proton transfer (ESIPT). By careful selection of the acidity and the hydrogen-bonding donor ability of the protons that are crucial to the ESIPT process, the above biologically interesting anions can be distinguished from the different spectral outputs for anion−sensor interactions.

Although inhibition of the ESIPT has been well exploited for cation sensing,[13] it was poorly applied for anion sensing.[14] In view of the attracting nature of the ESIPT and the knowledge of the hydrogen bond formation/neat proton transfer existing in the anion recognition processes gained by Fabbrizzi and co-workers[15] and more recently by us,[12] it is possible to develop new anion chemosensors based on the influence of anion binding on the ESIPT process. In the ESIPT molecules, the intramolecular hydrogen bonds (IHB) formed in the ground state between the hydrogen-bonding donors (e.g., −OH, $-NH_2$, etc.) and acceptors (=N−, >C=O, etc.) in close proximity are vital to the ESIPT process.[16] For example, in recent years the general family of 2-(2′-hydroxyphenyl)benzoxazole (HBO)[17] has been studied extensively to elucidate the mechanism of the ESIPT process, and the disturbances of the ESIPT in them have been ingeniously elaborated for sensing purposes. Deprotonation of the hydroxyl proton is the result of the coordination with lithium[13a] and zinc[13b] ions, or of the reaction with basic fluoride[14c] ions, so the ESIPT process is no longer possible, and a substantial blue shift in the peak emission would be expected. A wealth of information available about the photophysics of benzoxazole derivatives has prompted us to choose this class of molecules as an attractive starting point to explore the influence of anion binding on the ESIPT process.

SCHEME 1. Structure and Synthesis of Sensors TABO and PUBO

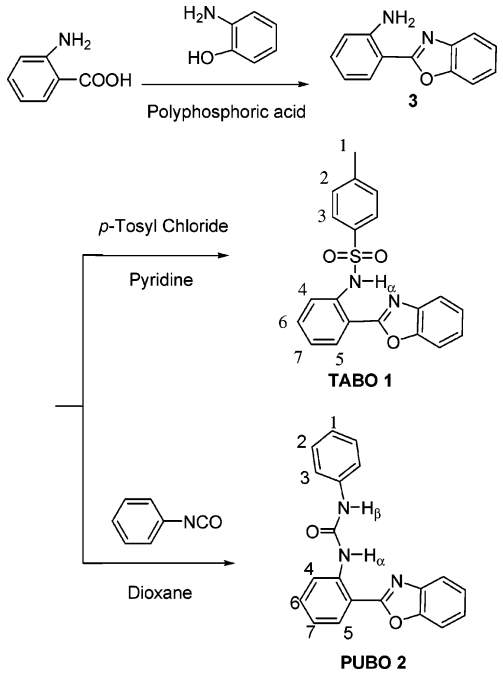

But for an anion sensor, if the sensing process is only based on proton transfer, the anion differentiation will definitely be poor, especially for the same spectral outputs with the addition of excess anions, due to the similar basicity and surface charge density of the anions.[5c,12] So in order to selectively differentiate the anions by utilizing the ESIPT mechanism, the anion receptor moieties of the newly designed sensors should have the following characteristics: receptor moieties should form IHB in the ground state with the adjacent hydrogen-bonding acceptors; the acidity of the receptors should be weak enough to avoid the deprotonation of sensors upon interaction with the basic anions such as F^- or CH_3COO^- but should be strong enough to induce a fast rate of ESIPT and increase the quantum yields of the tautomer emission Φ_{fl}^{T}.[18] In our new sensor 2-(2′-phenylureaphenyl)benzoxazole (PUBO, **2**, Scheme 1), the pK_a of the NH_α fragment in it satisfies the above requirements, which is higher than an −OH group[14] and lower than an $-NH_2$

(3) (a) Gunnlaugsson, T.; Kruger, P. E.; Jensen, P.; Tierney, J.; Ali, H. D. P.; Hussey, G. M. *J. Org. Chem.* **2005**, *70*, 10875−10878. (b) Gomez, D. E.; Fabbrizzi, L.; Licchelli, M.; Monzani, E. *Org. Biomol. Chem.* **2005**, *3*, 1495−1500. (c) Jose, D. A.; Kumar, D. K.; Ganguly, B.; Das, A. *Org. Lett.* **2004**, *6*, 3445−3448. (d) Lee, D. H.; Im, J. H.; Lee, J. H.; Hong, J. I. *Tetrahedron Lett.* **2002**, *43*, 9637−9640.

(4) (a) Kim, S. K.; Bok, J. H.; Bartsch, R. A.; Lee, J. Y.; Kim, J. S. *Org. Lett.* **2005**, *7*, 4839−4842. (b) Gale, P. A. *Chem. Commun.* **2005**, 3761−3772. (c) Camiolo, S.; Gale, P. A.; Hursthouse, M. B.; Light, M. E.; Warriner, C. N. *Tetrahedron Lett.* **2003**, *44*, 1367−1369.

(5) (a) Lee, D. H.; Lee, K. H.; Hong, J. I. *Org. Lett.* **2001**, *3*, 5−8. (b) Lee, D. H.; Lee, H. Y.; Lee, K. H.; Hong, J. I. *Chem. Commun.* **2001**, 1188−1189. (c) Zhang, X.; Guo, L.; Wu, F. Y.; Jiang, Y. B. *Org. Lett.* **2003**, *5*, 2667−2670.

(6) Chellappan, K.; Singh, N. J.; Hwang, I. C.; Lee, J. W.; Kim, K. S. *Angew. Chem., Int. Ed.* **2005**, *44*, 2899−2903.

(7) Sessler, J. L.; Camiolo, S.; Gale, P. A. *Coord. Chem. Rev.* **2003**, *240* (1−2), 17−55.

(8) (a) Wen, Z. C.; Jiang, Y. B. *Tetrahedron* **2004**, *60*, 11109−11115. (b) Wu, F. Y.; Li, Z.; Guo, L.; Wang, X.; Lin, M. H.; Zhao, Y. F.; Jiang, Y. B. *Org. Biomol. Chem.* **2006**, *4*, 624−630.

(9) (a) Thiagarajan, V.; Ramamurthy, P.; Thirumalai, D.; Ramakrishnan, V. T. *Org. Lett.* **2005**, *7*, 657−660. (b) Gunnlaugsson, T.; Ali, H. D. P.; Glynn, M.; Kruger, P. E.; Hussey, G. M.; Pfeffer, F. M.; dos Santos, C. M. G.; Tierney, J. *J. Fluoresc.* **2005**, *15*, 287−299.

(10) Sun, S. S.; Anspach, J. A.; Lees, A. J.; Zavalij, P. Y. *Organometallics* **2002**, *21*, 685−693.

(11) Wu, J. S.; Zhou, J. H.; Wang, P. F.; Zhang, X. H.; Wu, S. K. *Org. Lett.* **2005**, *7*, 2133−2136.

(12) Peng, X.; Wu, Y.; Fan, J.; Tian, M.; Han, K. *J. Org. Chem.* **2005**, *70*, 10524−10531.

(13) (a) Obare, S. O.; Murphy, C. J. *New J. Chem.* **2001**, *25*, 1600−1604. (b) Henary, M. M.; Fahrni, C. J. *J. Phys. Chem. A* **2002**, *106*, 5210−5220. (c) Fahrni, C. J.; Henary, M. M.; VanDerveer, D. G. *J. Phys. Chem. A* **2002**, *106*, 7655−7663. (d) Henary, M. M.; Wu, Y. G.; Fahrni, C. J. *Chem. Eur. J.* **2004**, *10*, 3015−3025. (e) Wu, K. C.; Lin, Y. S.; Yeh, Y. S.; Chen, C. Y.; Ahmed, M. O.; Chou, P. T.; Hon, Y. S. *Tetrahedron* **2004**, *60*, 11861−11868. (f) Taki, M.; Wolford, J. L.; O'Halloran, T. V. *J. Am. Chem. Soc.* **2004**, *126*, 712−713. (g) Zhang, X. B.; Peng, J.; He, C. L.; Shen, G. L.; Yu, R. Q. *Anal. Chim. Acta* **2006**, *567*, 189−195.

(14) (a) Tong, H.; Zhou, G.; Wang, L. X.; Jing, X. B.; Wang, F. S.; Zhang, J. P. *Tetrahedron Lett.* **2003**, *44*, 131−134. (b) Zhou, G.; Cheng, Y. X.; Wang, L. X.; Jing, X. B.; Wang, F. S. *Macromolecules* **2005**, *38*, 2148−2153. (c) Lee, J. K.; Na, J.; Kim, T. H.; Kim, Y. S.; Park, W. H.; Kim, J.; Lee, T. S. *Mater. Sci. Eng., C* **2004**, *24*, 261−264.

(15) (a) Boiocchi, M.; Del Boca, L.; Gomez, D. E.; Fabbrizzi, L.; Licchelli, M.; Monzani, E. *J. Am. Chem. Soc.* **2004**, *126*, 16507−16514. (b) Boiocchi, M.; Del Boca, L.; Esteban-Gomez, D.; Fabbrizzi, L.; Licchelli, M.; Monzani, E. *Chem. Eur. J.* **2005**, *11*, 3097−3104. (c) Amendola, V.; Esteban-Gomez, D.; Fabbrizzi, L.; Licchelli, M. *Acc. Chem. Res.* **2006**, *39*, 343−353.

(16) Schulman, S. G. Acid−Base Chemistry of Excited Singlet States. In *Modern Fluorescence Spectroscopy*; Wehry, E. L., Ed.; Plenum Press: New York, 1976; pp 239−275.

(17) (a) Das, K.; Sarkar, N.; Ghosh, A. K.; Majumdar, D.; Nath, D. N.; Bhattacharyya, K. *J. Phys. Chem.* **1994**, *98*, 9126−9132. (b) Roberts, E. L.; Dey, J.; Warner, I. M. *J. Phys. Chem.* **1996**, *100*, 19681−19686. (c) Rios, M. A.; Rios, M. C. *J. Phys. Chem. A* **1998**, *102*, 1560−1567.

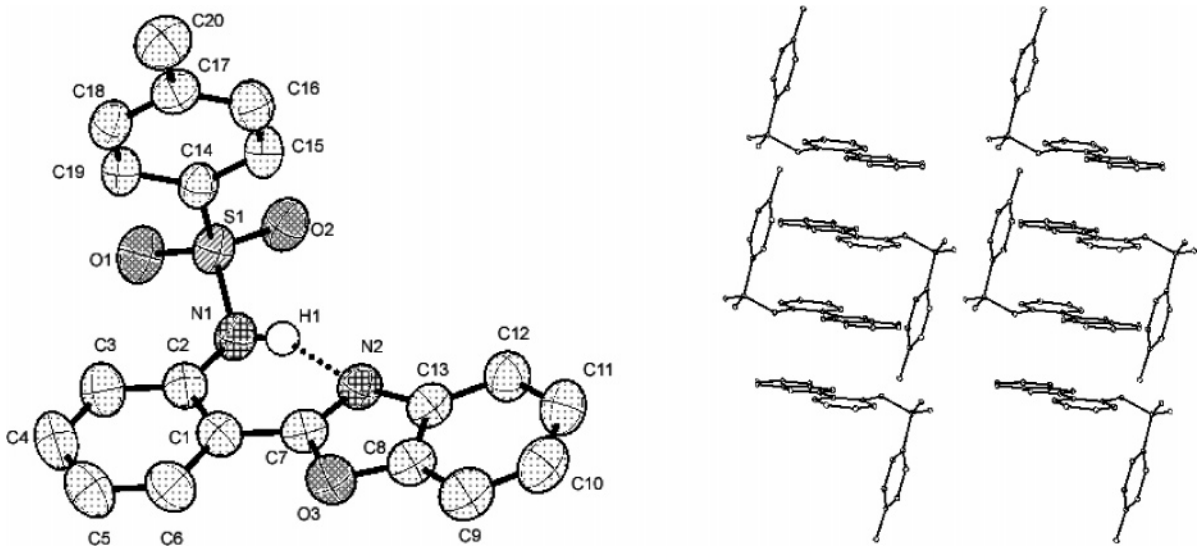

FIGURE 1. Left: ORTEP view of TABO showing the atomic numbering scheme. Thermal ellipsoids are drawn at the 50% probability level. Only the hydrogen atom involved in the intramolecular hydrogen bond is drawn, and other hydrogen atoms have been omitted for clarity. The dashed line indicates the hydrogen bond interaction. Right: Packing diagram of TABO exhibiting intermolecular $\pi-\pi$ stacking between the phenyl-benzoxazole units of two molecules.

group.[19] We also synthesized a relative acid receptor 2-(2′-tosylaminophenyl)benzoxazole (TABO, **1**), the pK_a of which is still higher than an −OH group, to investigate its anion sensitivity and selection. In particular, the sulfonamide subunit in TABO is more acidic than the urea subunit in PUBO, whereas the urea subunit in PUBO is a good hydrogen-bonding donor. The urea subunit can bind with single-acceptor anions, such as F^-, to yield a six-membered chelate ring, or it can bind with Y-shaped anions, such as CH_3COO^-, through the formation of two hydrogen bonds.[20] If the NH moieties of the ESIPT molecules interact with the anions, the ESIPT process can be inhibited either by the formation of the NH−anion hydrogen bond complex or by the deprotonation of NH_α by the more basic anions.

Results and Discussion

Synthesis. The syntheses of TABO and PUBO are shown in Scheme 1. First, the 2-(2′-aminophenyl)benzoxazole **3** was prepared in 68% yield according to a literature method,[21] then condensation of **3** with *p*-toluenesulfonyl chloride in pyridine at room temperature gave TABO in 95% yield, and with phenyl isocyanate in dry dioxane gave PUBO in 92% yield.

X-ray Structure Analysis of TABO. Crystals of TABO suitable for X-ray structural analysis were grown by slow evaporation of the TABO dichloromethane/ethanol solution. The most interesting feature of the structure (Figure 1) is the coplanarity of phenyl-benzoxazole unit with a small dihedral angle of 4.2°. This coplanarity is different from the reported geometry of a structurally similar ESIPT molecule, 2-(2′-tosylaminophenyl)benzimidazole.[13c] In 2-(2′-tosylaminophenyl)-benzimidazole, the intramolecular $\pi-\pi$ stacking interactions between the parallel orientation of the tosyl and benzimidazole rings induce a significant twist between the benzimidazole and phenyl rings with a big dihedral angle of 29°. The lack of the intramolecular $\pi-\pi$ stacking in TABO is compensated by the intermolecular π stacking between phenyl-benzoxazole units of two molecules, so the tosyl rings and the benzoxazole rings almost adopt a vertical orientation. A distance of 2.019(18) Å for N2−H1 reveals the H_α and the nitrogen on the benzoxazole ring form a strong IHB.[22] The coplanarity of the phenyl-benzoxazole unit and the strong IHB in TABO indicate the cis rotamer $\mathbf{E_c}$ (Scheme 2) is thermodynamically and substantially favored over other rotamers.

SCHEME 2. Possible Forms of Sensors in the Ground State and the Excited State in DMSO

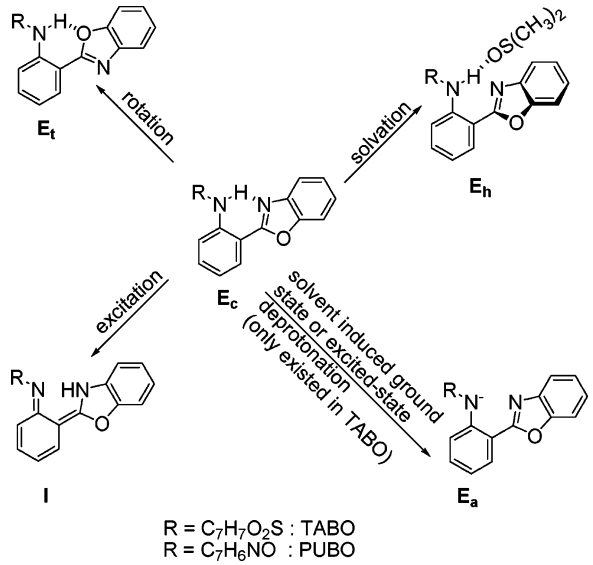

Photophysics of Sensors. The absorption spectra of TABO and PUBO were measured in different solvents. Their spectra are structured regardless of the solvent polarity (Figures 2 and 3), which are indicative of the rigidity of the molecular

(18) Santra, S.; Krishnamoorthy, G.; Dogra, S. K. *J. Phys. Chem. A* **2000**, *104*, 476−482.
(19) Santra, S.; Dogra, S. K. *Chem. Phys.* **1998**, *226*, 285−296.
(20) Hay, B. P.; Firman, T. K.; Moyer, B. A. *J. Am. Chem. Soc.* **2005**, *127*, 1810−1819.
(21) Hein, D. W.; Alheim, R. J.; Leavitt, J. J. *J. Am. Chem. Soc.* **1957**, *79*, 427−429.
(22) Desiraju, G. R., Ed. In *Crystal Design*: *Structure and Function*. *Perspectives in Supramolecular Chemistry*; Wiley-VCH: England, 2002.

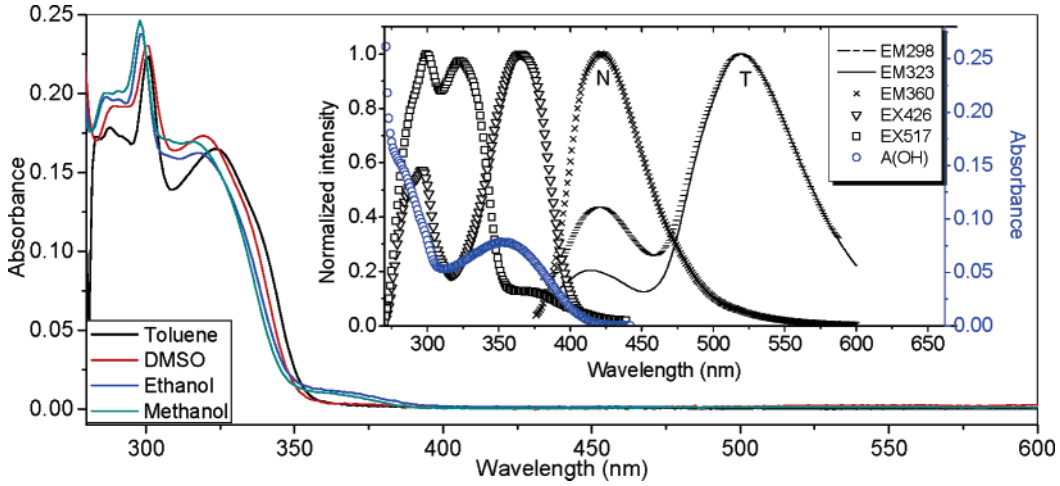

FIGURE 2. UV−vis absorption spectra of TABO (1.0×10^{-5} M) in various solvents. Inset: The normalized fluorescence excitation EX (▽, λ_{em} = 426 nm; □, λ_{em} = 517 nm) and emission EM (- - -, λ_{ex} = 298; —, λ_{ex} = 323 nm; ×, λ_{ex} = 360 nm) spectra for TABO in DMSO (N is the normal band and T is the tautomer band). The blue circle A(OH) is the UV−vis spectrum of TABO (1.0×10^{-5} M) in the presence of 10 equiv of $[(Bu)_4N]OH$.

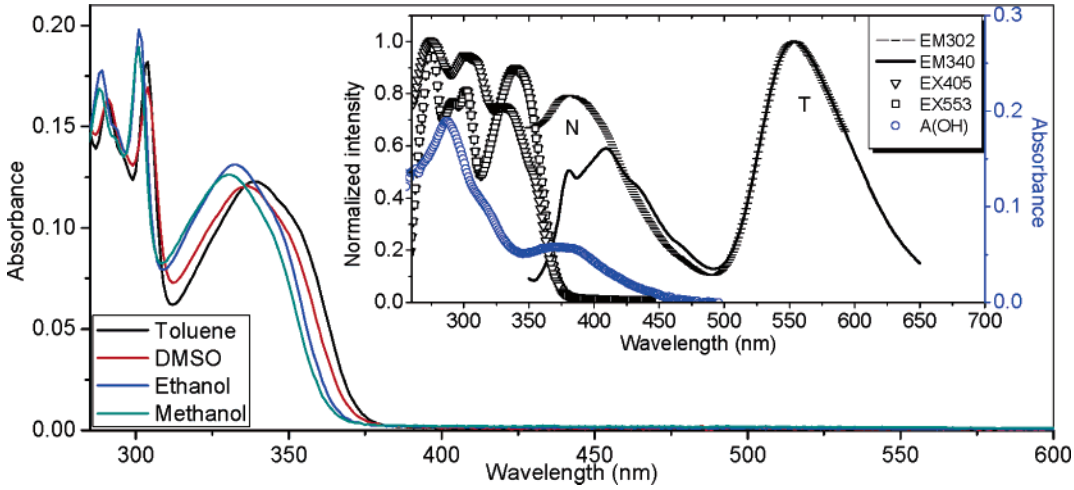

FIGURE 3. UV−vis absorption spectra of PUBO (1.0×10^{-5} M) in various solvents. Inset: The normalized fluorescence excitation EX (▽, λ_{em} = 405 nm; □, λ_{em} = 553 nm) and emission EM (- - -, λ_{ex} = 302; —, λ_{ex} = 340 nm) spectra for PUBO in DMSO (N is the normal band and T is the tautomer band). The blue circle A(OH) is the UV−vis spectrum of PUBO (1.0×10^{-5} M) in the presence of 10 equiv of $[(Bu)_4N]OH$.

TABLE 1. UV−vis Spectral Data (Absorption Maxima and Extinction Coefficients) and Fluorescence Spectral Data (λ_{ex} = 320 nm) for TABO in Various Solvents

solvent	λ_{max} (nm)	ϵ_{max} (M^{-1} cm^{-1})	λ_{max} (nm)	ϵ_{max} (M^{-1} cm^{-1})	λ_{max}^{fl} (N)[a]	Φ_{fl} (N)	λ_{max}^{fl} (T)[b]	Φ_{fl} (T)	Φ_T/Φ_N
cyclohexane	299	24021	324	15554	397	0.005	527	0.138	29
toluene	299	22191	322	16495	403	0.011	519	0.192	17
dichloromethane	300	25236	321	18456	413	0.013	507	0.323	25
DMSO	300	23037	319	17337	415	0.016	519	0.053	3
ethanol	299	23776	318	16246	420	0.022	508	0.160	7
methanol	298	24067	316	16963	419	0.018	506	0.092	5

[a] N = normal band. [b] T = tautomer band.

frameworks. Their absorption band maxima undergo slight blue shifts with the increasing of the polarity and hydrogen-bonding capacity of the solvents (Tables 1 and 2), which is the result of the partial breaking of the IHB with the formation of the NH_α−solvent hydrogen bond complex $\mathbf{E_h}$ (Scheme 2).[18] Another interesting feature is the appearance of a weak absorption band above 350 nm in TABO in polar protic solvents (Figure 2), which cannot be observed in PUBO (Figure 3). A similar weak absorption band has also been observed in 2-(2′-tosylaminophenyl)benzimidazole.[13c] This can be ascribed to the presence of small amounts of deprotonated ground-state anion $\mathbf{E_a}$ (Scheme 2). The acidic property of sulfonamide in TABO has made it easy to be deprotonated by the solvents with strong hydrogen-bonding acceptor abilities.

The fluorescence spectral data of TABO and PUBO were also measured in different solvents (Tables 1 and 2). Dual

TABLE 2. UV−vis Spectral Data (Absorption Maxima and Extinction Coefficients) and Fluorescence Spectral Data (λ_{ex} = 335 nm) for PUBO in Various Solvents

solvent	λ_{max} (nm)	ϵ_{max} (M^{-1} cm^{-1})	λ_{max} (nm)	ϵ_{max} (M^{-1} cm^{-1})	λ_{max}^{fl} (N)[a]	Φ_{fl} (N)	λ_{max}^{fl} (T)[b]	Φ_{fl} (T)	Φ_T/Φ_N
cyclohexane[c]	302		341		386	0.030	554	0.030	1.0
toluene	303	17972	340	12274	399	0.019	553	0.027	1.4
dichloromethane	302	18663	336	12481	387	0.014	549	0.033	2.4
DMSO	304	16938	336	12116	414	0.016	554	0.028	1.8
ethanol	301	19794	333	16246	391	0.008	545	0.025	3.3
methanol	301	18944	330	12635	401	0.010	543	0.017	1.7

[a] N = normal band. [b] T = tautomer band. [c] Determined in a saturated solution.

emissions are observed in all solvents: the normal emissions (blue fluorescence) and the large Stokes-shifted tautomer emissions (green fluorescence for TABO and yellow fluorescence for PUBO). With the increase of the polarity and hydrogen-bonding capacity of the solvents, the band maxima of the tautomer emissions get blue shifts, whereas the band maxima of the normal emissions get red shifts. The fact that Φ_T/Φ_N of TABO in DMSO decreases significantly when compared with that in cyclohexane indicates sulfonamide has a strong interaction with polar solvents, whereas Φ_T/Φ_N of PUBO becomes smaller and changes a little with the change of the solvents, which indicates the lower acidity of urea in PUBO not only reduces the tendency of the ESIPT process but also results in this ESIPT process resistance to the solvents' disturbances. The normal emission bands change with the excitation energy; for example, in TABO, when the excitation wavelengths change from 298 to 360 nm in DMSO, the normal emission band red shifts from 413 to 426 nm, which indicates at least two species such as $\mathbf{E_t}$ and $\mathbf{E_h}$ that are responsible for this observed emission band. Interestingly, excitation at a low energy of 360 nm gives a single emission band at 422 nm, and the excitation band recorded at 426 nm consists well with the weak absorption band in polar protic solvents (Figure 2) and the absorbance band formed in tetrabutyl ammonium hydroxide (inset of Figure 2, A(OH)). So it is presumed that the deprotonated excited anion species $\mathbf{E_a}$* exists in DMSO in the excited state though $\mathbf{E_a}$ cannot be detected from the absorbance in the ground state, whereas similar anion species $\mathbf{E_a}$* cannot be observed in PUBO from the excitation spectra recorded at different wavelengths (inset of Figure 3). So it can be deduced that the normal emission in PUBO is only the coaction results of two species: $\mathbf{E_t}$ and $\mathbf{E_h}$, whereas the tautomer emissions of TABO and PUBO are independent of the excitation wavelengths, and excitation spectra recorded at the tautomer emissions are structured, indicating that it is just the single quite rigid rotamer $\mathbf{E_c}$ responsible for these tautomer emissions. On the basis of the above analyses, it indicates that the ground-state equilibria of sensors in DMSO are dominated by $\mathbf{E_c}$ and the normal bands are the combination results of $\mathbf{E_t}$ and $\mathbf{E_h}$, or possibly $\mathbf{E_a}$, and the excited-state intermolecular proton transfer[23] between NH_α and DMSO can also make a contribution in TABO if the excitation is chosen at a low energy, but the tautomer bands only derive from $\mathbf{E_c}$ (Scheme 2).

Anion Sensing in the Ground State. The interactions of sensors with anions were investigated through spectrophotometric titrations by adding a standard solution of the tetrabutylammonium salt of anions to a dry DMSO solution of sensors. Figure 4 shows the UV−vis spectral changes of TABO during the titration with F^-. Addition of F^- induces the formation of

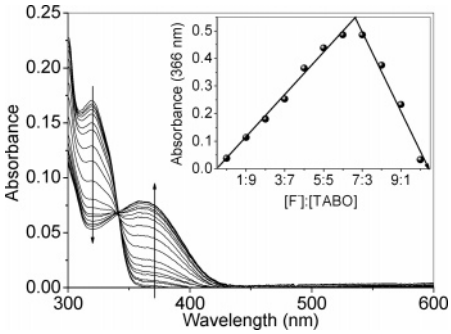

FIGURE 4. Changes in the UV−vis spectra for TABO (1.0×10^{-5} M) in DMSO with the addition of $[(Bu)_4N]F$ from 0 to 0.0005 M. Inset: Job's plot for fluoride−TABO interactions. The total $[F^-]$ + [TABO] = 2.0×10^{-4} M.

a new red-shifted absorption band at 360 nm with the decrease of the band at 320 nm. This new band matches well with the absorption band formed in tetrabutyl ammonium hydroxide (inset of Figure 2, (AOH)), so it derives from the deprotonated anion species $\mathbf{E_a}$. Though there exists an isosbestic point at 341 nm, the stoichiometry of the fluoride−TABO interactions is confirmed to be 2:1 from the Job's plot (inset of Figure 4). Analogous investigations were also carried out on a variety of anions such as $CH_3CO_2^-$, $H_2PO_4^-$, HSO_4^-, Cl^-, and Br^-. Only $CH_3CO_2^-$ and $H_2PO_4^-$ induced similar spectral changes (Figure S1 in the Supporting Information), but the spectral responses from $H_2PO_4^-$ were not as sensitive as F^- and $CH_3CO_2^-$.

A ^1H NMR titration experiment in DMSO-d_6 was conducted to further investigate the fluoride−TABO interactions in the ground state, as shown in the partial ^1H NMR F^- titration spectra of TABO in Figure 5. Upon addition of 0.5 molar equiv of F^-, the majority of signals on the phenyl rings shift distinctly upfield owing to charge delocalization on the entire conjugated system with the deprotonation of TABO, and the signal for the NH_α proton (11.5 ppm) can still be detected at this time. With increasing F^-, the phenyl signals shift upfield further, and these shifts stop after the addition of F^- up to 2 molar equiv, which also indicates TABO−fluoride interactions follow 1:2 stoichiometry. From the entire titration, it can be seen that the deprotonation process takes place upon addition of F^- and dominates the entire titration. So this deprotonation process can be expressed by the following Brönsted acid−base reaction equilibrium (1).

$$LH + F^- \overset{K_d}{\rightleftharpoons} L^- + FH \qquad (1)$$

The above equilibrium indicates that only one equiv of F^- reacts with TABO to form a deprotonated species. But from the Job's plot, a stoichiometry of 1:2 is observed for TABO−

(23) Agmon, N. *J. Phys. Chem. A* **2005**, *109*, 13−35.

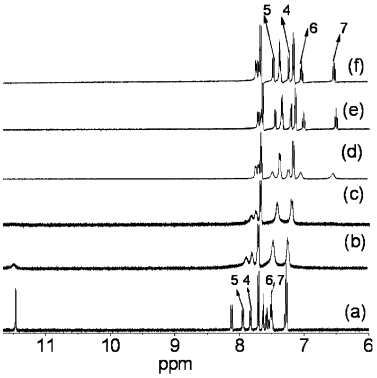

FIGURE 5. Partial ^{1}H NMR (400 MHz) spectra of TABO (1.0×10^{-2} M) in DMSO-d_6 in the absence (a) and the presence of 0.5 (b), 1.0 (c), 2.0 (d), 4.0 (e), and 7.0 (f) equiv of $[(Bu)_4N]F$ (proton labeling shown in Scheme 1).

fluoride interactions. By considering the particular high stability of the FHF^- dimer,[12] it can be concluded that the following dimer formation process occurs in the subsequent step.

$$FH + F^- \rightleftharpoons FHF^- \tag{2}$$

Combining eqs 1 and 2, the overall equilibrium can be obtained, which indicates a stoichiometry of 1:2 for TABO−fluoride interactions.

$$LH + 2F^- \rightleftharpoons L^- + FHF^- \tag{3}$$

This two-step process can also be applied to the anions $CH_3CO_2^-$ and $H_2PO_4^-$, which can form relatively stable dimers,[15b] because a stoichiometry of 1:2 was also observed for TABO−anion interactions (Figure S2 in the Supporting Information). On the other hand, though Cl^- cannot induce an observable spectral change in absorbance (Figure S3a in the Supporting Information), a genuine hydrogen bond interaction (eq 4) between sulfonamide and Cl^- can be detected from the NMR Cl^- titration spectra (Figure S3b).

$$LH + Cl^- \overset{K_a}{\rightleftharpoons} [LH\cdots Cl]^- \tag{4}$$

However, urea−fluoride interactions in PUBO are slightly different from sulfonamide−fluoride interactions in TABO. With the addition of F^- up to 216 molar equiv, the entire UV−vis absorbance bands of PUBO increase slightly, but an obvious absorption change is observed with the further addition of 5 more molar equiv F^-, and then the absorption band at 336 nm decreases gradually accompanying the formation of a new band at 385 nm with the further addition of F^- (Figure 6). These stepwise changes in F^- titration spectra are well consistent with previous reports about urea−fluoride interactions,[15] so it can be concluded that PUBO−fluoride interactions are also a two-step process, but the entire process can be expressed by the following two equilibria.[15]

$$LH + F^- \overset{K_a}{\rightleftharpoons} [LH\cdots F]^- \tag{5}$$

$$[LH\cdots F]^- + F^- \overset{K_d}{\rightleftharpoons} L^- + FHF^- \tag{6}$$

The first step is hydrogen bond formation (eq 5), which produces minimal disturbance on the dipole associated with the charge-transfer transition of sensor PUBO, and consequently

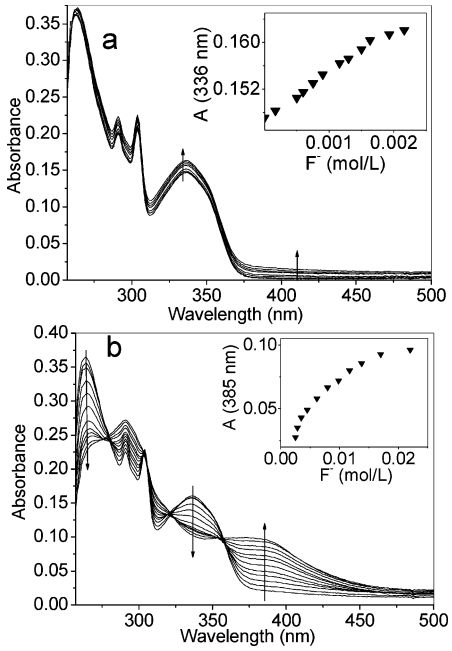

FIGURE 6. Changes in the UV−vis spectra for PUBO (1.0×10^{-5} M) in DMSO with the addition of $[(Bu)_4N]F$ (a) from 0 to 0.002 M and (b) from 0.002 to 0.022 M.

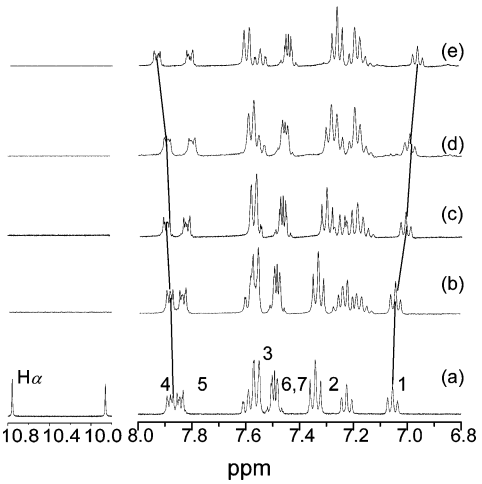

FIGURE 7. Partial ^{1}H NMR (400 MHz) spectra of PUBO (1.0×10^{-2} M) in DMSO-d_6 in the absence (a) and the presence of 0.5 (b), 2.0 (c), 4.0 (d), and 7.0 (e) equiv of $[(Bu)_4N]F$ (proton labeling shown in Scheme 1).

only a small change is observed in the UV−vis spectra, then the second step produces a deprotonation species (eq 6). With the charge redistribution taking place within the deprotonated species, the UV−vis spectra exhibit a red-shifted charge-transfer (CT) band.

The ^{1}H NMR F^- titration experiment in PUBO can also support the hydrogen bond formation in the first step (Figure 7). For the ^{1}H NMR titration spectrum, two effects are responsible for the spectral changes upon NH−anion hydrogen bond formation:[15a] (1) through-bond effects, which increase the electron density of the phenyl ring and promote upfield shifts, and (2) through-space effects, which polarize the C−H bond in proximity to hydrogen bonds, create partial positive charge on the proton, and cause downfield shifts. Upon addition of 0.5 molar equiv of F^-, the complete disappearance of the signals

TABLE 3. Log *K* for TABO and PUBO Interaction with Anions

	TABO		PUBO			
anion	log K_d[a]	log K_d[b]	log K_a[a]	log K_a[b]	log K_d[a]	log K_d[b]
F^-	4.39 ± 0.10	4.35 ± 0.04	2.92 ± 0.07	3.02 ± 0.08	2.06 ± 0.09	2.09 ± 0.08
$CH_3CO_2^-$	4.39 ± 0.08	4.30 ± 0.08	2.00 ± 0.03	2.10 ± 0.07		
$H_2PO_4^-$	3.31 ± 0.15	3.29 ± 0.16	1.80 ± 0.10	1.91 ± 0.10		

[a] From UV−vis titration spectra. [b] From fluorescence titration spectra.

of the urea subunit protons (9.9 and 10.8 ppm) is observed. According to the spectral changes with the further addition of the F^- from 2 to 7 molar equiv, the protons can be classified as two categories: the first group is the protons that shift downfield with the increase of F^-, whereas the second is those that shift upfield. For the protons that are in proximity to hydrogen bonds (protons 3 and 4), the through-space effects dominate, so the downfield shift of the first group of protons is observed. However, for the protons that are far from the hydrogen bonds (protons 1, 2, 5, 6, and 7), the through-bond effects take action and the protons shift upfield. Due to the suppression of the phenyl signals with the addition of a further amount of F^-, the deprotonation of urea which occurs in the second step cannot be observed from the ^{1}H NMR titration experiment, but this deprotonation process can also be proved from the identical UV−vis spectral changes in the titration experiment with tetrabutylammonium hydroxide as that with F^- (inset of Figure 3, (AOH)).

It is interesting that the two types of hydrogen-bonding donors in TABO and PUBO follow different interaction mechanisms with F^- in the ground state. The reason for these differences lies in the difference between the acidity and hydrogen bond formation ability in sulfonamide and urea. The acidity and poor hydrogen-bonding donor ability of sulfonamide have made it easy to be deprotonated by the basic acceptors. But for the good hydrogen-bonding donor, urea in PUBO can only be deprotonated by F^- in the second step due to the exceptionally high stability of the FHF^- dimer, whereas for the Y-shaped anions CH_3COO^- and $H_2PO_4^-$, they can form a hydrogen bond complex with PUBO during the entire UV−vis titration (Figure S4 in the Supporting Information).

Anion Inhibition of the ESIPT. The above discussions show that strong bases such as F^-, $CH_3CO_2^-$, and $H_2PO_4^-$ can easily remove the sulfonamide proton in TABO to form $\mathbf{E_a}$ in the ground state. So the fluorescence anion titration spectra are expected to experience the disappearance of the normal and tautomer emission in favor of the deprotonation emission $\mathbf{E_a}$. The fluorescence responses of the TABO interaction with F^- were recorded with an excitation at the absorption band maximum of 320 nm for the purpose of avoiding the disturbance from the excited-state intermolecular proton transfer between TABO and DMSO. It is interesting that this deprotonation induces a great fluorescence enhancement (Figure 8). The emission of $\mathbf{E_a}$ lies just between the normal and tautomer emission and buries them quickly with the addition of F^-. As what was exhibited in the absorbance titration spectra, $CH_3CO_2^-$, and $H_2PO_4^-$ can also induce similar spectral changes (Figure S5 in the Supporting Information). For the weak base Cl^-, though it cannot induce obvious spectral change in absorbance (Figure S3a), it can induce a significant fluorescence decrease, especially for the tautomer emission (Figure S3c), which is an indication of the ESIPT in TABO inhibited by the sulfonamide−chloride hydrogen bond formation.

It should be noted that a major cause of fluorescence quenching−internal conversion exists in the free sensor TABO due to its low quantum yields in solutions (Table 1), which can be enhanced by both intra- and intermolecular hydrogen bonds.[24] With the fluoride-induced elimination of the IHB that associates with the rapid internal conversion, the quantum yields of the deprotonated species of TABO increase, whereas for the chloride-induced fluorescence quenching, it can be explained that the intermolecular hydrogen bond between sulfonamide and Cl^- can compete with the IHB to inhibit the ESIPT, so a significant quenching of the tautomer emission is observed during the Cl^- titration. In addition, due to the newly formed intermolecular hydrogen bond being another source of internal conversion, the normal emission also quenches a little.

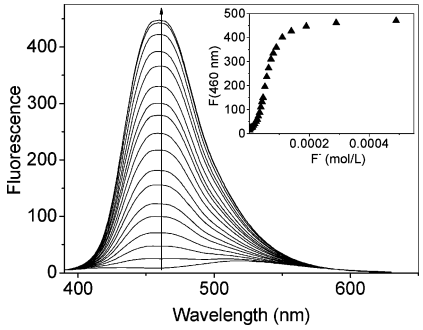

FIGURE 8. Changes in the fluorescence spectra (λ_{ex} = 320 nm) for TABO (1.0×10^{-5} M) in DMSO with the addition of a standard solution of $[(Bu)_4N]F$ from 0 to 0.0005 M. Inset: Fluorescence change at 460 nm vs concentration of F^-.

So for the basic anions, inhibition of the ESIPT in TABO is just the result of the elimination of the sulfonamide proton that is critical to the ESIPT process. From the anion titration spectra, the proton dissociation constants (log K_d, eq 1) are calculated and compiled in Table 3. Though the ESIPT can readily be disturbed by this deprotonation, the resulting spectral outputs are same both for the absorbance and the fluorescence. In other words, the sensitivity is good, but the distinguishability is poor. This is especially true for F^- and $CH_3CO_2^-$ with similar big equilibrium constants, so from the titration spectra, we cannot distinguish these two anions. Then we turn to the less acidic but good hydrogen-bonding donor receptor, PUBO, to investigate its anion distinguishability.

The fluorescence responses of PUBO interaction with F^- were recorded with an excitation at the isosbestic point of 322 nm. Similar to the UV−vis titration spectra (Figure 6), fluorescence titration spectra of PUBO with F^- also take on a stepwise change (Figure 9). Fluoride has little disturbance on fluorescence of PUBO in the first step. With the further addition of F^-, a new broad emission band appears, which derives from the deprotonated species $\mathbf{E_a}$ and also lies in the middle of the normal and the tautomer emission. Interestingly, the fluorescence titration spectra experience a ratiometric response in the second step. It is known that the IHB between the hydrogen-bonding donors

(24) Flom, S. R.; Barbra, P. F. *J. Phys. Chem.* **1985**, *89*, 4489−4494.

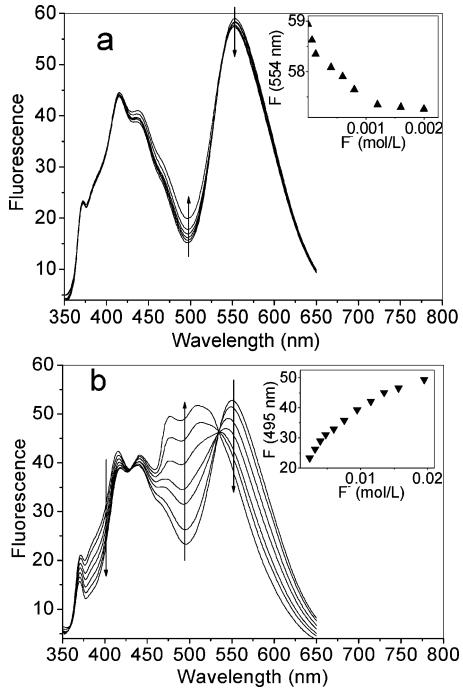

FIGURE 9. Changes in the fluorescence spectra (λ_{ex} = 322 nm) for PUBO (1.0×10^{-5} M) in DMSO upon the addition of a standard solution of $[(Bu)_4N]F$ (a) from 0 to 0.002 M and (b) from 0.002 to 0.022 M.

and the hydrogen-bonding acceptors could enhance the acidity of the donors,[25] so it can be concluded that it is the NH_α proton that is deprotonated in the second step (Table of Contents graphic). Just like the TABO, the inhibition of ESIPT in PUBO by F^- is also the result of the elimination of the proton that is crucial to the ESIPT

When the sensor PUBO was titrated with the Y-shaped anion CH_3COO^-, different spectroscopic patterns were obtained. During the UV−vis titration (Figure S4a), a slight blue shift and decrease in absorption band at 336 nm are observed; however, no red-shifted CT band is developed even after the addition of an excess of CH_3COO^-. The facts that the titration spectra only experience a one-step change and there exist well-defined isosbestic points at 330 nm indicate CH_3COO^- can only form a hydrogen bond with the urea subunit of PUBO during the entire titration. This intermolecular hydrogen bond formation can disturb the IHB and destroy the rigidity of the $\mathbf{E_c}$, so the blue shift and decrease in the absorption band at 336 nm are observed. The corresponding fluorescence titration spectra (Figure 10) also experience a significant ratiometric response when excited at the isosbestic point of 330 nm: the decrease of the tautomer emission band at 554 nm accompanies with the increase of the normal emission band at 414 nm, and this ratiometric fluorescence response is fully different from that of the F^- titration. These fluorescence spectral changes are the result of, with the twist of the phenyl-benzoxazole unit induced by the strong CH_3COO^-−urea hydrogen bond (Table of Contents graphic), the decreasing of $\mathbf{E_c}$ with the increasing of $\mathbf{E_h}$. Though the tautomer band can be efficiently inhibited by CH_3COO^-, it still can be detected even after the addition of excess anion, suggesting the IHB in PUBO is exceptional strong.

(25) Chen, X.; Walthall, D. A.; Brauman, J. I. *J. Am. Chem. Soc.* **2004**, *126*, 12614−12620.

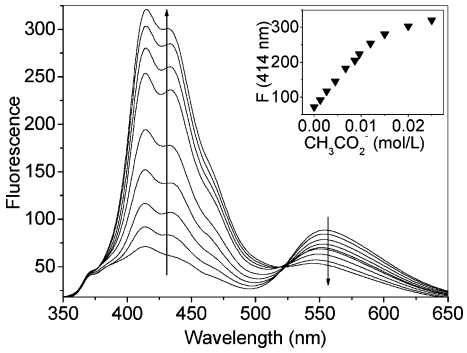

FIGURE 10. Changes in the fluorescence spectra (λ_{ex} = 330 nm) for PUBO (1.0×10^{-5} M) in DMSO with the addition of $[(Bu)_4N]CH_3CO_2$ from 0 to 0.025 M.

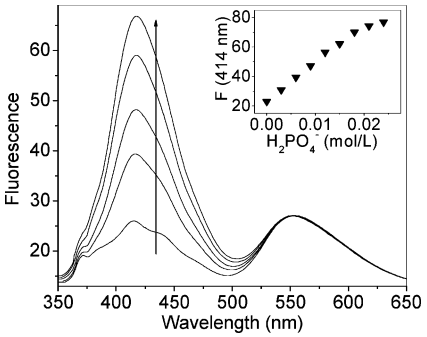

FIGURE 11. Changes in the fluorescence spectra (λ_{ex} = 336 nm) for PUBO (1.0×10^{-5} M) in DMSO with the addition of $[(Bu)_4N]H_2PO_4$ from 0 to 0.025 M.

Spectral titrations were also conducted with the less basic anions such as Cl^-, Br^-, I^-, HSO_4^-, and $H_2PO_4^-$. Only $H_2PO_4^-$ can induce the distinct spectral changes, and also different spectra results are obtained. The intensity of absorption increases slightly with the addition of the $H_2PO_4^-$, and the shape of the absorption band does not change during the entire titration (Figure S4b), which indicate the formation of the $H_2PO_4^-$−urea hydrogen bond complex. As for the fluorescence titration spectra (Figure 11), though the normal band increases significantly with the increase of the $H_2PO_4^-$, the tautomer band does not decrease at all during the titration. The above behaviors are ascribed to the much lower basicity and less hydrogen-bonding acceptor property of $H_2PO_4^-$ with respect to those of F^- and CH_3COO^-. The hydrogen bonds between the urea subunit and $H_2PO_4^-$ are no longer strong enough to destroy the strong IHB in $\mathbf{E_c}$ and suppress the ESIPT process, whereas the $H_2PO_4^-$-induced fluorescence enhancement of the normal band may be a consequence of an increase in the rigidity of the sensor molecule upon anion complexation, which decreases the probability of nonradiative decay in the excited state, and therefore could enhance the quantum yields and the intensity of the normal emission.[1d]

From the fluorescence changes described above, it is should be noted that, though equilibrium constants (log *K*) are similar for these three anions interaction with PUBO (Table 3), the inhibition mechanisms exerted by them are really different. It is found that the basicity, shape, and hydrogen-bonding acceptor properties of anions determinate their abilities to inhibit the ESIPT. Due to the exceptional deprotonation ability with the formation of particular high stability of the FHF^- dimer, F^- inhibits the ESIPT by deprotonating the IHB that is vital to the

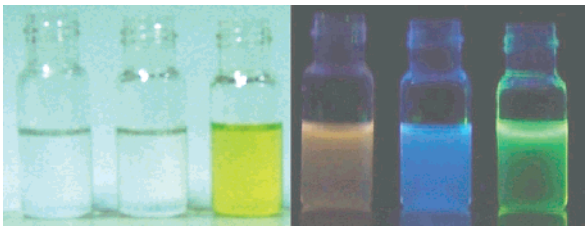

FIGURE 12. Color and fluorescence changes of PUBO in DMSO (2.0×10^{-4} M) after addition of 0.01 M of anions. Left to right: PUBO, PUBO + $[(Bu)_4N]CH_3CO_2$, PUBO + $[(Bu)_4N]F$, PUBO (emission), PUBO + $[(Bu)_4N]CH_3CO_2$ (emission), and PUBO + $[(Bu)_4N]F$ (emission). Irradiation at 365 nm using a UV lamp.

ESIPT process, whereas for CH_3COO^-, the strong intermolecular hydrogen bonding between the CH_3COO^- and urea induces a twist in the benzodazole and phenyl ring, so the tautomer emission is expected to decrease with the increasing of the emission from $\mathbf{E_h}$. For $H_2PO_4^-$, the ESIPT could not be inhibited due to its less basic and hydrogen-bonding acceptor ability. More importantly, the different inhibition abilities of F^-, CH_3COO^-, and $H_2PO_4^-$ produce different spectral behaviors (Figure 12). So the new ESIPT-based sensor PUBO successfully distinguishes the subtle difference in these three anionic substrates of similar basicity and surface charge density. It also should be noted that, due to the sensors based on other mechanisms often experiencing red shifts with the addition of anions,[12] the blue shifts in fluorescence for anion−sensor interactions are unique in the ESIPT sensors.

From the spectral outputs for sensors interaction with anions described above, it can be found that the acidity and hydrogen-bonding donor ability of NH_α are also decisive factors to control the inhibition mechanisms, and different inhibition mechanisms consequently give different spectral outputs. In view of the anion sensitivity and distinguishability in TABO and PUBO, TABO has more sensitivity but less distinguishability, and vice versa for PUBO. The anion differentiation of PUBO is based on the different spectral outputs. TABO, however, gives the same spectral outputs after interaction with anions, so the anion differentiation of TABO is only based on the different binding constants. In view of the convenience of detection, PUBO (with different spectral outputs) will be more useful than TABO (with different binding constants).

Conclusion

In conclusion, we have presented a new kind of fluorescent anion sensor based on inhibition of the excited-state intramolecular proton process. By varying the acidity and the hydrogen-bonding donor ability of the protons that are crucial to the ESIPT process, a combination of a good sensitivity and distinguishability will definitely be obtained. Importantly, the sensor design principle and the correlation between the properties of anions and their abilities to inhibit the ESIPT will be a very useful clue to design more delicate ESIPT-based chemosensors.

Experimental Section

2-(Benzo[*d*]oxazol-2-yl)benzenamine (3). Compound **3** was prepared according to a literature method.[21] Mp 106−107 °C (lit.[26] 105 °C). HRMS *m*/*z* (TOF MS ES$^+$) calcd for $C_{13}H_{11}N_2O^+$ ([M + H]$^+$), 211.0871; found, 211.0874.

***N*-(2-(Benzo[*d*]oxazol-2-yl)phenyl)-4-methylbenzenesulfonamide (TABO).** *p*-Toluenesulfonyl chloride (400 mg, 2.1 mmol) was added to a solution of compound **3** (420 mg, 2 mmol) in dry pyridine (10 mL) in a round flask filled with argon at room temperature, and the mixture was stirred for 10 h. The mixture was poured into H_2O (20 mL), neutralized with HCl (1 M), and extracted with dichloromethane (2 × 20 mL). The combined organic phase was washed with H_2O (2 × 20 mL), dried with $MgSO_4$, filtered, and purified by flash column chromatography on silica gel with dichloromethane as eluent to afford a white solid (690 mg, 95%). Mp 165−166 °C. δ_H (400 MHz; DMSO-d_6; Me_4Si): 2.02 (s, 3H), 7.26−7.30 (m, 3H), 7.48−7.52 (m, 2H), 7.58 (d, 1H, J = 8.4 Hz), 7.63 (d, 1H, J = 8.4 Hz), 7.71 (d, 2H, J = 8.0 Hz), 7.82−7.84 (m, 1H), 7.93−7.95 (m, 1H), 8.12 (d, 1H, J = 8.4 Hz), 11.46 (s, 1H). δ_C (400 MHz; DMSO-d_6; Me_4Si): 21.6, 110.7, 113.8, 119.1, 120.2, 123.3, 125.2, 126.0, 127.4, 128.7, 129.7, 132.7, 136.7, 138.3, 140.7, 143.9, 149.3, 161.6. HRMS *m*/*z* (TOF MS ES$^+$) calcd for $C_{20}H_{16}N_2NaO_3S^+$ ([M + Na]$^+$), 387.0779; found, 387.0786.

1-(2-(Benzo[*d*]oxazol-2-yl)phenyl)-3-phenylurea (PUBO). Phenyl isocyanate (250 mg, 2.1 mmol) was added to a solution of compound **3** (420 mg, 2 mmol) in dry dioxane (50 mL) in a round flask filled with argon. The mixture was heated at 100 °C under magnetic stirring for 24 h. After the reaction mixture was cooled to room temperature, a white solid precipitated. Then the crude compound was collected by filtration, dried, and recrystallized from dioxane to afford the pure product **1** as a white solid (605 mg, 92%). Mp 200−202 °C. δ_H (400 MHz; DMSO-d_6; Me_4Si): 7.04 (t, 1H, J = 7.2 Hz), 7.21 (t, 1H, J = 7.2 Hz), 7.34 (t, 2H, J = 7.2 Hz), 7.48−7.50 (m, 2H), 7.56−7.60 (m, 3H), 7.84−7.88 (m, 2H), 8.18 (d, 1H, J = 8.0 Hz), 8.43 (d, 1H, J = 8.8 Hz), 9.85 (s, 1H), 10.75 (s, 1H). δ_C (400 MHz; DMSO-d_6; Me_4Si): 111.0, 112.1, 119.4, 119.7, 120.3, 121.7, 122.5, 125.1, 125.9, 128.4, 128.8, 132.5, 139.5, 139.7, 140.5, 148.9, 152.4, 161.4. HRMS *m*/*z* (TOF MS ES$^+$) calcd for $C_{20}H_{15}N_3NaO_2^+$ ([M + Na]$^+$), 352.1062; found, 352.1057.

Acknowledgment. This work was supported by the National Natural Science Foundation of China (Projects 20376010, 20472012, and 20642003).

Supporting Information Available: Determination of quantum yields; crystal data of TABO (CIF); determination of equilibrium constants; absorbance titration spectra of TABO with the addition of CH_3COO^- and $H_2PO_4^-$; Job's plot for TABO interaction with CH_3COO^-; absorbance, ^1H NMR, and fluorescence titration spectra of TABO with the addition of Cl^-; absorbance titration spectra of PUBO with the addition of CH_3COO^- and $H_2PO_4^-$; fluorescence titration spectra of TABO with the addition of CH_3COO^- and $H_2PO_4^-$; $^1H-^1H$ COSY spectra of TABO and PUBO. This material is available free of charge via the Internet at http://pubs.acs.org.

JO061634C

(26) Haskell, T. H.; Peterson, F. E.; Watson, D.; Plessas, N. R.; Culbertson, T. *J. Med. Chem.* **1970**, *13*, 697−704.